Optimization-Based Reconstruction of Depolarization of the Heart

D Farina[1], O Skipa[1], C Kaltwasser[2], O Dössel[1], WR Bauer[2]

[1]Institute of Biomedical Engineering, Universität Karlsruhe (TH), Germany
[2]University Clinical Centre, Würzbug, Germany

Abstract

A new noninvasive method to obtain a priori data for solving the inverse problem of electrocardiography is suggested. The method employs a personalized 3D model of the patient built from MRI data and an electrophysiological model of the patient's heart (cellular automaton).

The distribution of body surface potentials is calculated. The simulated ECG is "recorded" and compared with that measured for the patient. The parameter values of the cellular automaton are optimized in order to obtain the best possible correspondence between measured and simulated ECGs.

The method provides a set of distributions of transmembrane voltages in the myocardium. These distributions can be used as a priori data for other types of inverse problems in electrocardiography. In this way valuable information about the cardiac electrical activity is obtained.

1. Introduction

The inverse problem of electrocardiography aims to reconstruct the electrical activity within the myocardium from multichannel ECG. Solving it is a new promising way to avoid invasive intrusion for diagnostics of heart diseases. A serious complication is that the problem is *ill-posed*, i.e. arbitrary small noise in ECG signals can lead to arbitrary large errors in reconstructed cardiac activity.

To get round this problem, a number of regularization methods have been developed. They apply *a priori* constraints to the solution, in order to stabilize it (see, e.g, [1]). A typical constraint is applied, for example, on the amplitude of the solution, limiting therefore its integral energy. Sometimes several types of constraints are used simultaneously [2].

An important way to improve the reconstruction quality is to insert an initial approximation of the result into the formulation of regularization. In this work we obtain the data for such an estimation based on the solution of the forward problem of electrocardiography, which includes a personalized electrophysiological model of a patient.

It should be mentioned, that the application of the forward problem to improve the quality of reconstruction using the inverse problem was also studied, e.g., in [3]. The use of transmembrane voltage source formulation of the forward problem to improve the regularization quality was approved in [4, 5].

2. Methods

The following steps were undertaken in order to obtain the distributions of transmembrane voltages within the heart, that most correctly describe the measured ECG. First, a personalized model of the thorax of the patient was built using MRI-scans. Second, a cellular automaton was run on the anatomical model of the patient's heart, simulating the excitation propagation inside the myocardium. Using a bidomain model, resulting transmembrane voltages were converted into the current sources. Next, a body surface potential map (BSPM) was built for each state of cellular automaton, i.e. for each generated distribution of transmembrane voltages. The last step was to save the potentials at the points of the model, which corresponded to the positions of electrodes during the measurement of ECG on the real patient.

In this way the simulated ECG was obtained. It was compared with the measured ECG, previously filtered and with corrected zero line. A root-mean-square of the difference was calculated for each of the channels and afterwards averaged. The resulting value was taken as a criterion for optimization.

In the following subsections these steps are described in more detail.

2.1. Volume conductor model

The model of the volume conductor was built on the basis of MR-images, measured with Siemens Magnetom Vision MRI-scanner at the University of Würzburg, Germany. A typical image had a resolution of approximately 4x4x4mm. Organs such as lungs, liver and fat were segmented to ensure the right spatial

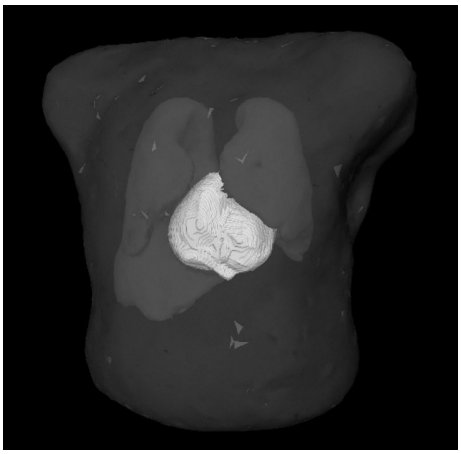

Figure 1. A simplified model of the volume conductor. Lungs, heart, liver are shown.

distribution of amplitudes of signals on the body surface. The segmentation was done using a software package, previously developed at the Institute of Biomedical Engineering, Universität Karlsruhe (TH).

It will be shown later, that in spite of our efforts to generate the best possible model of the patient's thorax, amplitude correction had to be used in order to suppress the effects, caused by the discrepancy of electrical conductivity distributions in the model and in the human body.

In order to receive more detailed information about the heart of the patient, MRI-scans with better resolution (typically 2x2x4mm) were made for the heart region. As the global coordinate system was the same for all types of the images, the correspondence between the locations of the heart, segmented from such scans, and of the whole thorax could be easily found.

A typical volume conductor model is shown in Fig. 1.

2.2. Simulation of cardiac activity

The model of the heart used for simulations included the following components, which were included based on the physiologic rules:

- AV-Node
- Bundle branches
- Left and right ventricles
- Blood contained in ventricles.

The ventricles and blood were segmented from MR-images using deformable triangle meshes. Then a 3D data set with cubic voxels of 1mm size was created. Cellular automaton was run on this data set, in order to simulate the propagation of depolarization wave through the heart tissue. The information on the cellular automaton used in this work can be found in more detail in [6, 7].

The resolution of MR-images did not allow to segment the atria, so the role of excitation generator was given to the AV-node. Then the excitation propagated through the bundle branches to the ventricles and afterwards through the myocardium, producing the QRS-complex of the electrocardiogram.

Each distribution of transmembrane voltages was transformed into the distribution of current sources using the bidomain model. Then the latter distribution was interpolated to the irregular tetrahedron mesh, representing the model of the thorax. BSPMs were calculated using the finite element method [8].

2.3. Comparison

The distribution of body surface potentials of patients was measured using the 64-channel device manufactured by BioSemi (Amsterdam, Netherlands). The electrode positions were measured using Polhemus Fastrack (Polhemus Inc., Vermont, USA). The latter were used to bring the measured and simulated ECGs into correspondence.

The volume conductor of the human thorax smoothes and attenuates the signal generated by the wave of depolarization. In spite of using a rather complicated model of human thorax, the level of attenuation caused by the real human thorax was not achieved. In other words, the amplitude of the simulated ECGs on the electrodes, distant from the heart, was much higher than that of the measured ECG. As the main aim was to correct the parameters of the heart model, and not that of the volume conductor, the amplitudes were normalized using the following formula:

$$A_{norm} = diag\left\{ \left| \frac{b_{i,max}}{a_{i,max}} \right| \right\} \cdot A, \qquad (1)$$

here A and B are the matrices of the simulated and measured ECGs, respectively. Their rows represent a time dependent signal on a single electrode, their columns represent body surface potential maps. The $a_{i,max}$ and $b_{i,max}$ symbols designate the amplitude of R-peak on the channel i of simulated and measured ECGs, respectively.

This operation brings the amplitude of R-peak for each channel of simulated ECG to that of the measured ECG, in other words, we trace only the differences in the form of the QRS-complex, and not the difference in its amplitude. In this way we avoid the necessity to take into account the distortion, introduced by the improper volume conductor model.

The root-mean-square of the difference between measured and simulated QRS-complexes was calculated for each channel according to the usual definition:

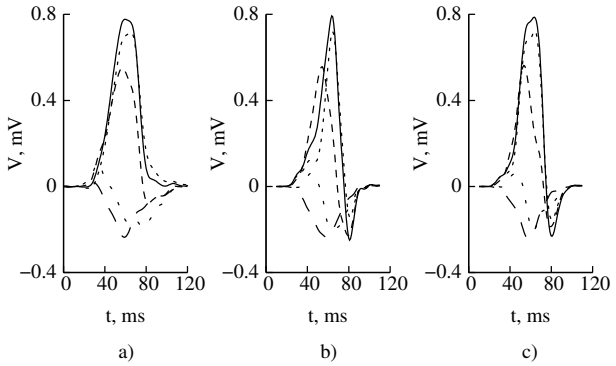

Figure 2. QRS-complex for 5 of 64 electrodes: measured (a), simulated (b), simulated optimized (c)

$$RMS_i = \sqrt{\frac{\sum_{j=1}^{N}(a_{ij} - b_{ij})^2}{N}}. \quad (2)$$

Here i is a counter for channels, j for indices, N designates the amount of samples taking part in the comparison on each channel; a_{ij} and b_{ij} are the elements of matrices A_{norm} and B from equation (1), respectively.

As the parameter characterizing the deviation of the simulated ECG from the measured one, the average RMS over all the channels was chosen:

$$DEV = \frac{\sum_{i=1}^{CN} RMS_i}{CN}. \quad (3)$$

Here CN stands for the number of channels.

2.4. Optimization

The parameter DEV, obtained from equation (3), was used as a criterion for optimization. The parameters, which should be optimized, were chosen to be the speed of excitation propagation in each class of bundle branches, such as Tawara nodes in right and left ventricles, as well as anterior and posterior fascicles in the left ventricle and Purkinje fibers in both ventricles. The space of varied parameters was therefore limited by 6 dimensions. This approach allowed us to control the time at which the excitation passed through the bundle branches and reached the myocardium.

For the optimization a Powell's method was chosen, as it is described in [9].

3. Results

Due to the multitasking structure of the optimization software, a double speed on each simulation of BSPM is achieved. (On a PowerMac G5 workstation with two 64-bit processors a normal, single-tasking calculation of a set of BSPMs during a single heart beat with a step of 4 ms took about 400 s, whereas the multitasking variant completed the calculation in 240 s.)

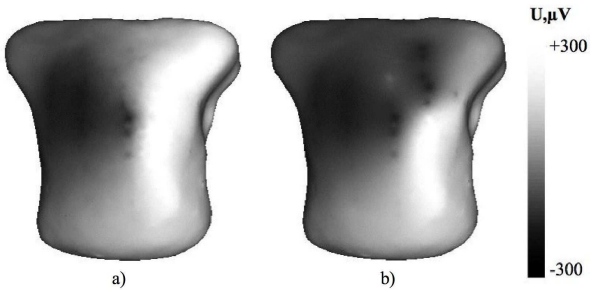

Figure 3. BSPMs: measured (a), simulated (b). Time point corresponds to $t = 50ms$ in Fig. 2.

The process of optimization resulted in the decrease of the deviation parameter (see eq.(3)) by 30-50%. On the contrary, the change of parameters of the model during the optimization never exceeded 15% of the values found in literature. Although the parameters do not carry any special diagnostic information, this proves good correspondence between the model and the reality.

The difference between original and optimized simulated ECGs is shown in Fig.2 (b, c) – to be compared with measured ECG in Fig.2 (a).

The measured and simulated distributions of the body surface potentials are presented for comparison in Fig. 3 (a, b). Considerable differences, appearing here at the left shoulder, can be eliminated with more careful construction of the heart model. The rest of the thorax surface shows good correspondence between simulated and measured potentials.

4. Discussion and conclusions

The method being presented in this work delivers the time dependence and spatial distribution of transmembrane voltages within the heart tissue. This estimation can be used to solve a number of types of inverse problems.

The parameters being varied here are the velocities of excitation propagation within different tissue classes. Nevertheless it's not a limitation of present method: almost any kind of parameters can be varied in the same way.

Recently a possibility to optimize the position of infarction in the left ventricle was introduced. The parameters for optimization here are the spherical coordinates (θ and φ) of the infarction relatively to the geometrical centre of the left ventricle and its main axis, as well as its size in mm. On the moment of writing this article, the calculations on the first patient were held, and the right position of infarction was already found.

The results of estimation are shown in Fig. 4 (a). Special

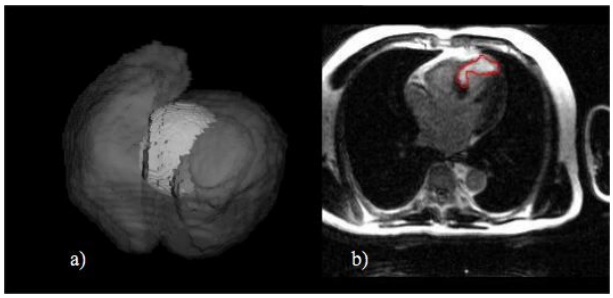

Figure 4. Site and size of a myocardial scar: (a) after optimized reconstruction; (b) as detected by contrast-enhanced MR-imaging (late-enhancement)

MR-images of the patient – with an MR contrast agent revealing the myocardial scar – were provided to control the quality of reconstruction. Such an image is shown in Fig. 4 (b). On both images the scar is located in the septum and has approximately the same size.

This preliminary result indicates, that the method is able to provide the physician with important diagnostic data. Extended e.g. with a technique for solving linear inverse problems, this method can be a powerful tool for the diagnostics of heart diseases.

Acknowledgements

This work was supported by German Research Association.

References

[1] Hansen C. Rank-deficient and discrete ill-posed problems: numerical aspects of linear inversion. SIAM, Philadelphia, 1998.

[2] Brooks DH, Ahmad GF, MacLeod RS, Maratos GM. Inverse electrocardiography by simultaneous imposition of multiple constraints. IEEE Trans Biomed Eng 1999;46:3–18.

[3] He B, Li G, Zhang X. Noninvasive imaging of cardiac transmembrane potentials within three-dimensional myocardium by means of a realistic geometry anisotropic heart model. IEEE Trans Biomed Eng 2003;50:1190–1202.

[4] Messnarz B, Tilg B, Modre R, Fischer G, Hanser F. A new spatiotemporal regularization approach for reconstruction of cardiac transmembrane potential patterns. IEEE Trans Biomed Eng 2004;51:273–281.

[5] Messnarz B, Seger M, Modre R, Fischer G, Hanser F, Tilg B. A comparison of noninvasive reconstruction of epicardial versus transmembrane potentials in consideration of the null space. IEEE Trans Biomed Eng 2004;51:1609–1618.

[6] Werner C. Simulation der elektrischen Erregungsausbreitung in anatomischen Herzmodellen mit adaptiven Zellulaeren Automaten. Tenea, Berlin, 2001.

[7] Werner CD, Sachse FB, Doessel O. Electrical excitation propagation in the human heart. Int J Bioelectromagnetism 2000;2.

[8] Skipa O. Linear inverse problem of electrocardiography: epicardial potentials and transmembrane voltages. Helmesverlag Karlsruhe, 2004.

[9] Press WH, Teukolsky SA, Vetterling WT, Flannery BP. Numerical recipes in C: the art of scientific computing. Second edition. Cambridge University Press, 1992.

Address for correspondence:

Dmitry Farina
Institute of Biomedical Engineering
University of Karlsruhe
Kaiserstraße 12
76128 Karlsruhe Germany
email: df@ibt.uni-karlsruhe.de